Papers

Long period oscillations in the longshore current on a sandy, barred coast investigated with Singular Spectrum Analysis*

OCEANOLOGIA, 47 (1), 2005.
pp. 5–25.

KEYWORDS
Longshore current
Singular spectrum analysis
Nearshore hydrodynamics
Infragravity waves
Beach processes

Jarosława Kaczmarek
Grzegorz Różyński*
Zbigniew Pruszak

Institute of Hydroengineering,
Polish Academy of Sciences,
Kościerska 7, PL–80–953 Gdańsk, Poland;

e-mail: grzegorz@ibwpan.gda.pl

*corresponding author

Received 13 December 2004, revised 11 February 2005, accepted 14 February 2005.

Abstract

The presence of infragravity waves in nearshore regions can be sought in the records of both water levels and wave-driven longshore currents. For this reason, time series of such currents in close proximity to the shoreline were analysed using Singular Spectrum Analysis (SSA). Simultaneously, the results obtained with this method were confronted with the output of Discrete Wavelet Transform (DWT), which had previously been applied to this data. The records of longshore currents were collected on a daily basis during field experiments in the autumns of 2002 and 2003 with sampling rates of 3 Hz and 0.5 Hz. This produced a large data set that allowed for the use of an advanced signal processing technique, capable of extracting patterns characteristic of low-, medium- and high-frequency bands. It

* This study was conducted within the framework of grant No 5T07A 019 24, funded by the Committee of Scientific Research (KBN) and as part of the Institute of Hydroengineering PAS's (IBW PAN) statutory activities.

provided similar evidence to that produced by DWT for the existence of infragravity waves along a dissipative coast with multiple bars. The study also demonstrated the utility of SSA for studies on coastal hydrodynamics. It also showed up the better user-friendliness of DWT in terms of pattern extraction and interpretation. On the other hand, SSA demonstrated a higher precision of pattern extraction once the DWT output was known, which is a manifestation of the synergy of the two methods when applied jointly.

1. Introduction

Coastal processes are characterised by complex, nonlinear phenomena; they also involve patterns covering a wide range of spatial and temporal scales (De Vriend 1991, Larson & Kraus 1995). Even though substantial progress has been achieved in the investigation of physical mechanisms driving coastal morphodynamic processes, present knowledge remains insufficient to correctly understand, model, and forecast the behaviour of many coastal systems (Stive et al. 2002). One way to achieve a better understanding of the evolution of nearshore morphodynamics is to focus on hydrodynamics, which is the major driver of changes in coastal morphology. However, the lack of good quality hydrodynamic data has prevented applications of state-of-the-art signal processing techniques in data-driven hydrodynamic investigations, despite their well-established reputation gained in a number of studies on nearshore morphology (see e.g. Winant et al. 1975, Wijnberg & Terwindt 1995, Reeve et al. 2001). Notable exceptions are data from long-established national tide-gauge networks (see e.g. Aubrey & Emery 1983, Solow 1987, Ding et al. 2001) used for tidal harmonic decomposition and surge analysis. Still, the vast majority of data-driven investigations is based on the scrutiny of morphological patterns only. Even though these patterns result from all forcings, couplings and feedbacks, the effects of changes in hydrodynamics cannot be elicited from them.

The Coastal Research Station (CRS) at Lubiatowo, Poland, is no exception to this rule. The morphology of this beach, which lies on the southern Baltic Sea (Fig. 1), is characterised by multiple sandbars (Fig. 2), and features a highly dissipative and purely wave-driven system. As such, it is shaped by variations in wave-driven hydrodynamics, mostly during extreme events when, apart from wave action, storm surges and wave-generated nearshore currents largely contribute to morphological evolution. Such changes have been recorded for many years, providing data sets on nearshore bed topography and shoreline evolution. Measurements of nearshore bed topography have been performed twice a year, gaining geodetic compatibility in 1987. Records of shoreline configurations have been collected on a monthly basis since September 1983 and were geodetically referenced from the moment they started. In recent years these data sets

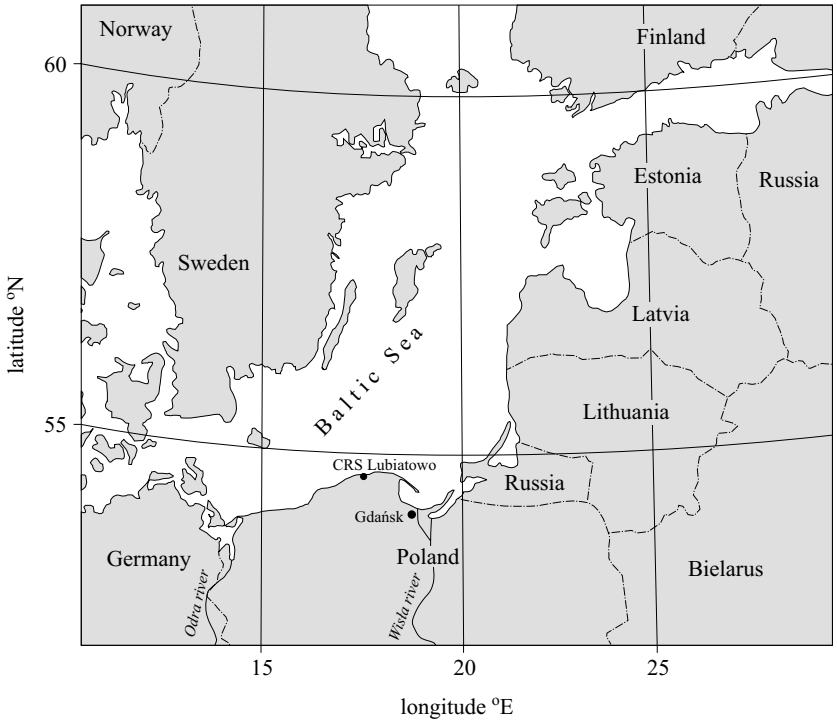

Fig. 1. CRS Lubiatowo – geographical location

have been subjected to extensive analysis with modern statistical techniques. Singular Spectrum Analysis (SSA) was employed to trace forced and self-organised components of shoreline change (see Różyński et al. 2001, Reeve 2002). Principal Oscillation Patterns (POP) were used to derive a data-driven model of changes in nearshore bathymetry (Różyński & Jansen 2002). Empirical Orthogonal Functions (EOF) and Canonical Correlation Analysis (CCA) were combined to study interactions among inner and outer bars (Różyński 2003). Finally, multi-channel SSA (MSSA) was utilised to improve the understanding of shoreline variability originating from an ordinary SSA study (Różyński 2005). Exploration of these morphological data sets appears to have reached a limit now and a more profound insight into the evolution of non-tidal, sandy, barred beaches calls for the analysis of hydrodynamic data. Such data were also collected at Lubiatowo during field experiments. The measurements included the records of deep- and shallow-water waves at different cross-shore locations of the nearshore zone in order to capture wave-transformation and wave-energy dissipation patterns. They also embraced wave-driven longshore and cross-shore currents so that physical models of such currents in a system with multiple bars could be

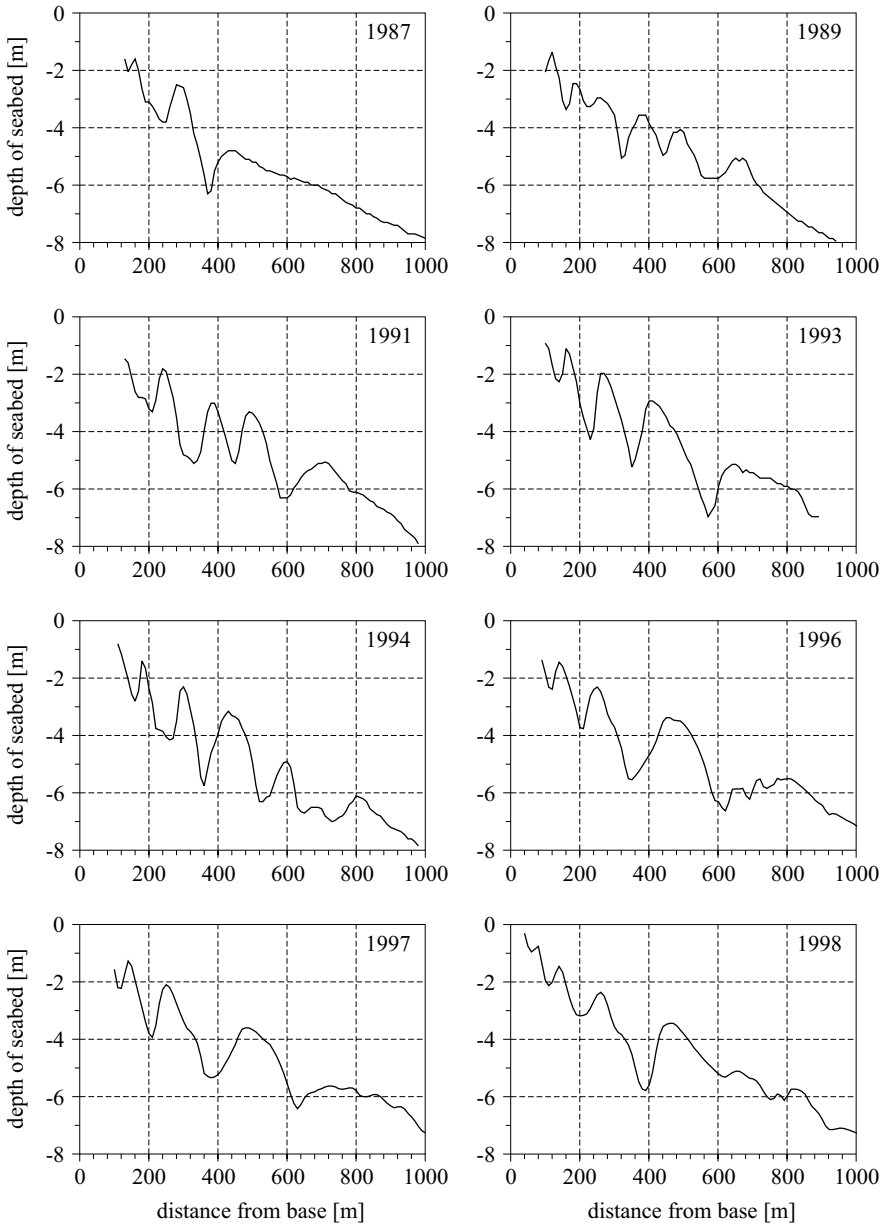

Fig. 2. Examples of nearshore seabed configurations at CRS Lubiatowo

studied (Szmytkiewicz 2002). In 2002 and 2003 field experiments were targeted towards the identification and description of infragravity waves, which are believed to be responsible for the formation of various shoreline morphological forms. Therefore, a wave gauge and current meters were

placed some 20–30 m offshore. The data sets thereby acquired allowed for in-depth studies using modern statistical tools for hydrodynamic processes in that part of the nearshore region. For this purpose the SSA method was first used to search for and extract slow-varying components in the time series of water levels in an attempt to discover the existence of patterns that could represent infragravity waves (Pruszak et al., in press). The promising results of that study were the inspiration for the application of Discrete Wavelet Transform (DWT) to the simultaneous analysis of the water-level and longshore current time series during an extreme event in order to find out how the potential presence of infragravity waves is imprinted in the variations of the longshore current (Różyński & Reeve, submitted).

The present study is intended to reveal long-period components in the longshore currents with the SSA method, as was done with the records of the water table, in order to either confirm or deny the relation between components with similar periods in the two series. In this way the extent to which slow variations in the water table are imprinted in the series of longshore currents will be examined with two methods. Such an investigation is very interesting, because it enables the comparison of two methods, based upon different assumptions, which have been developed for the extraction of patterns from data. The DWT method can resolve a raw signal into orthogonal components containing different spectral bands, defined and fixed by the sampling rate of a series. Note that this technique requires no assumption of stationarity. The variations of significance of these bands throughout the examined series is easily seen in the DWT output, so this method offers an excellent means for studying non-stationary data. This merit of wavelets in marine sciences was highlighted by Massel (2001), who applied wavelet analysis to the records of deepwater waves breaking over tropical coral reefs, and by Huang (2004), who investigated the use of wavelets as a means of filtering time series to extract wave parameters. On the other hand, the SSA method does assume time series stationarity, but puts no constraints on spectral band limits in the patterns it generates. Successful application of this technique to the analysis of water level variations and to the extraction of rhythmic shoreline features (Pruszak et al., in press) provides grounds for postulating that it should also perform well when studying the behaviour of longshore currents. In this way, two powerful signal processing techniques can be compared. Moreover, the analysis with two methods can provide more solid evidence for the existence of infragravity waves on a predominantly dissipative, barred coast. Hence, the key objectives of this paper are:

(1) To decompose characteristic records of longshore currents with the SSA method in order to extract key patterns, similar to those obtained when long-term variations of water level were analysed.

(2) To search for the impact of the presence in the longshore current series of infragravity waves detected in the water level series.

(3) To compare the performance of DWT and SSA as a means of extracting patterns in hydrodynamic data, with special emphasis on the potential presence of infragravity waves.

The remainder of the text begins with a description of the field site at the Lubiatowo beach in Poland and of the hydrodynamic data collected during the last two major field experiments. This is followed by an outline of the SSA method, and then a presentation of the SSA-based analysis of the longshore current time series. Next comes a comparison of the performance of DWT and SSA. The paper ends with conclusions and recommendations for future uses of intensive signal processing of hydrodynamic data in coastal engineering.

2. Field site and data collected

The Institute of Hydroengineering PAS (IBW PAN) Coastal Research Station is situated at Lubiatowo on the Polish coast on the southern Baltic Sea (see Fig. 1). The beach is usually characterised by multiple longshore bars and has a gentle mean slope of $\tan\beta = 1$–1.5% with a median grain size of $D_{50} = 0.22$ mm. Since the resulting long-term energy flux is oblique to the shore, a predominantly west to east littoral drift is observed. Multiple breakers are commonly encountered in the surf zone. Long-term records indicate that for average storms the significant wave height outside the surf zone (in water of depth h around 20 m) generally reaches $H_s = 2$–2.5 m with a mean period of $T = 5$–7 s. The incoming wave energy is dissipated as the waves move onshore, and for $h = 2$–3 m the mean height typically equals $\overline{H} = 0.5$–1 m with $T = 4$–5 s (Pruszak et al. 1999). Closer to the shoreline ($h = 1$ m) the height of the waves during storms reduces to 0.3–0.5 m. Since the Baltic Sea is virtually isolated from the Atlantic Ocean there is no influence from tides. The average surf similarity parameter, defined as $\xi = \tan\beta/\sqrt{H_0/L_0}$, where H_0 and L_0 represent deepwater wave height and length respectively, generally falls below 0.1 owing to the gently sloping bottom, which indicates that the coast at Lubiatowo is a highly dissipative system.

Long-term bathymetric surveys have shown that the beach at CRS Lubiatowo normally includes a system of four stable bars (see Fig. 2). The innermost bar is situated about 120–170 m from the baseline with

a water depth over the crest of ∼1 m, the second at 220–300 m with a water depth over the crest of ∼2 m, the third at 400–500 m and water depth over the crest of between 3 and 3.5 m, and the fourth, outermost bar is located at 600–800 m and a water depth over the crest of 4–5 m. At times a short-lived bar develops in the vicinity of the shoreline, typically located some 20–80 m from the baseline. The permanent bars do not migrate, but only oscillate around their average locations (Pruszak et al. 1997, 1999).

Hydrodynamic data were collected during a number of field experiments in the 1970s, 80s and 90s. They were usually carried out in the autumn, because most extreme events occur during this season. Wave gauges and current meters were deployed at measuring towers, initially covering the whole cross-shore span of the nearshore region. The gauges recorded wave transformation patterns over the multiple bars, whereas the meters traced water velocities over bar crests and within troughs. The sampling rate of those measurements was usually 10 Hz, so the records generally reflected the action of wind waves. The offshore towers have been subjected to gradual destruction by ice action and at present only the two innermost towers remain operational. In 2002 new field experiments were launched, which aimed to identify and describe infragravity waves in a multi-bar environment. For this reason an extra steel rod was driven into the seabed about 30 m offshore, where the average seabed depth hovers around 0.5 m. Afterwards, a wave gauge and two current meters were deployed there. One of the latter recorded longshore water velocities, the other cross-shore water velocities. In 2002 their sampling rate was initially set at 0.5 Hz; in 2003 this was raised to 3 Hz for one month, after which it reverted to the original rate of 0.5 Hz. This allowed for the collection of time series of water levels and nearshore currents. The volume of data acquired is large enough to support studies on various aspects of nearshore hydrodynamics for several years at least. The monitoring details are summarised in Table 1.

Table 1. Records of water level, longshore and cross-shore current in close shoreline proximity

2002		2003	
Date	Remarks	Date	Remarks
Oct. 23–28 Oct. 30–Nov. 3	23.5 hours continuous record, sampling rate 0.5 Hz	Sept. 17–19 Sept. 21–Oct. 16	4 times 6 hours continuous record, sampling rate 3 Hz
		Oct. 17–20 Oct. 22 Oct. 24–Nov. 13 Nov. 15	23.5 hours continuous record, sampling rate 0.5 Hz

3. Singular spectrum analysis (SSA)

As a result of the pioneering work by Vautard et al. (1992), Singular Spectrum analysis became a respectable tool of pattern extraction in the 1990s. In marine sciences it was successfully applied by Różyński et al. (2001) to extract forced and self-organised shoreline behaviour at Lubiatowo. For this reason only a brief description of the methodology is provided below.

SSA investigates the eigenstructure of a lagged covariance matrix of the time series x_i, where $1 <= i <= N$. This matrix is symmetrical and has constant terms on its diagonals:

$$T_x = \begin{bmatrix} c(0) & c(1) & ... & c(M-1) \\ c(1) & c(0) & c(1) & . \\ . & c(1) & c(0) & . \\ c(M-1) & ... & c(1) & c(0) \end{bmatrix}, \tag{1}$$

where

$$c(j) = \frac{1}{N-j} \sum_{i=1}^{N-j} (x_i - \overline{x})(x_{i+j} - \overline{x}), \tag{2}$$

and $\overline{x}$ is the mean value of this time series. The number M is the user-defined *embedding dimension.* To avoid unacceptable statistical errors in (2) for large j, M should be no greater than $\frac{1}{3}N$.

The matrix (1) has only positive terms on the main diagonal, so all its eigenvalues λ_k are positive. The corresponding eigenvectors E^k are orthogonal. The eigenvectors form the time-invariant part of the SSA decomposition, whereas the variability of a given system is contained in the *principal components* (PCs) – these, to a certain extent, are analogous to the well-known EOF principal components. The k-th PC is the projection coefficient of the original signal onto the k-th eigenvector:

$$a_i^k = \sum_{j=1}^{M} x_{i+j-1} E_j^k, \qquad 1 \le i \le N - M + 1. \tag{3}$$

According to (3) we have to take M elements of the x series from the i-th to $i + M$-th element, compute their products with the corresponding elements of the k-th (column) eigenvector and sum them to obtain the i-th element of the k-th PC. Hence, the PCs are time series of the length N–M. Formally, although the PCs are orthogonal to each other, they are not independent, because in (3) M consecutive elements of the original time series are needed to compute one term of every PC. Thus, there are k common elements of this series for the i-th term of the r-th PC a_i^r and the j-th term of the s-th PC a_j^s, such that $k = M - |j - i| > 0$ (lag $|j - i|$).

Hence, the correlation structure of the original series is imprinted in the sequence of the PC terms.

The PCs do not provide a unique expansion of the signal into a sum of different components. Using the PCs we can expand our series as

$$x_{i+j} = \sum_{k=1}^{M} a_i^k E_k^j, \qquad 1 \le j \le M. \tag{4}$$

There may be up to M subsets of the original time series containing the specific element x_{i+j}. Therefore, there are up to M different ways of reconstructing the components of the signal with (4) which do not produce the same results. It is possible, though, to construct a least-square optimum series corresponding to a given (sub)set of the eigenelements. If the following expression is minimised,

$$H_\Psi(y) = \sum_{i=1}^{N-M+1} \sum_{j=1}^{M} (y_{i+j} - \sum_{k\in\Psi} a_i^k E_j^k)^2, \tag{5}$$

where y is the desired series and Ψ is the subset of eigenelements, the solution $y = R_\Psi x$ is given by

$$(R_\Psi x)_i = \frac{1}{M} \sum_{j=1}^{M} \sum_{k\in\Psi} a_{i-j+1}^k E_j^k \qquad \text{for} \quad M \le i \le N-M+1, \tag{6a}$$

$$(R_\Psi x)_i = \frac{1}{i} \sum_{j=1}^{i} \sum_{k\in\Psi} a_{i-j+1}^k E_j^k \qquad \text{for} \quad 1 \le i \le M-1, \tag{6b}$$

$$(R_\Psi x)_i = \frac{1}{N-i+1} \sum_{j=1-N+M}^{M} \sum_{k\in\Psi} a_{i-j+1}^k E_j^k \qquad \text{for} \quad N-M+2 \le i \le N. \tag{6c}$$

If Ψ contains only a single index k, the resulting series is called the k-th *reconstructed component* (RC), which is denoted by x^k, and the RCs are additive, i.e. $R_\Psi x = \sum_{k\in\Psi} x^k$. Hence, the series x can be *uniquely* expanded as the sum of its RCs:

$$x = \sum_{k=1}^{M} x^k. \tag{7}$$

Since the RCs are correlated, the variances of RCs are not cumulative. Each RC has N elements. Usually, all useful information is contained in only a few RCs associated with the greatest eigenvalues of the SSA system matrix defined by (1). RCs are the sought-after SSA patterns, whose behaviour requires interpretation, which is often possible without any *a priori* knowledge of the physical background of the underlying system.

4. SSA analysis of wave-driven longshore current

For the analysis of patterns in the longshore current at CRS Lubiatowo the record of October 27th, 2002 was selected (Fig. 3). The same series was investigated with multi-resolution analysis (DWT) (see Table 2), so the SSA output allows for immediate comparison of the two methods. As can be seen

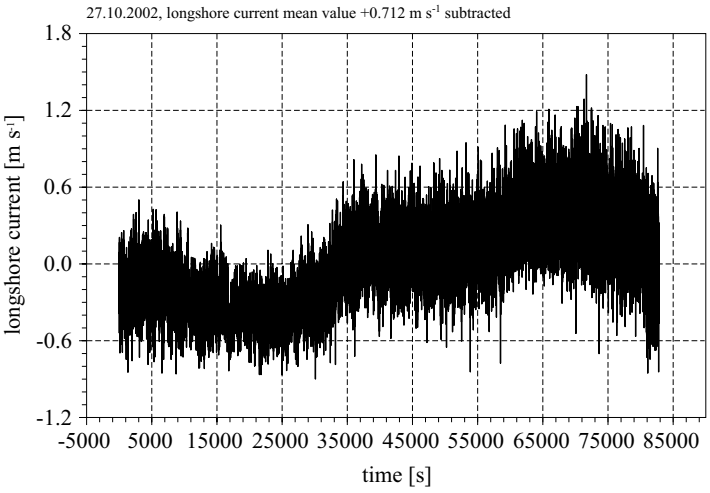

Fig. 3. Analysed longshore current series

Table 2. Breakdown of variation among wavelet components of longshore current series

Component	Spectral band	SD [m s^{-1}]	Percentage of variation	Remarks
Raw series		0.3256	100	
trend	$T > 4096$ s	0.264	65.5	variances of com-
D1	$4 < T < 8$ s	0.11	11.5	ponents cumula-
D2	$8 < T < 16$ s	0.083	6.5	tive, patterns
D3	$16 < T < 32$ s	0.064	3.8	orthogonal and
D4	$32 < T < 64$ s	0.055	2.9	uncorrelated
D5	$64 < T < 128$ s	0.05	2.4	
D6	$128 < T < 256$ s	0.048	2.0	
D7	$256 < T < 512$ s	0.044	1.8	
D8	$512 < T < 1024$ s	0.040	1.5	
D9	$1024 < T < 2048$ s	0.032	0.9	
D10	$2048 < T < 4096$ s		0.7	

SD – standard deviation.

from Fig. 3, this graph illustrates the rapid growth of longshore velocities over almost 24 hours, which manifests a stormy event, typical of the Baltic coast at the end of October. This series is centred about its mean value of 0.712 m s^{-1}, so in reality it represents the predominantly unidirectional flow of water from west to east. Fig. 4 contains its spectrum and rightly shows that most of the energy is stored in the ultra-low frequency band, corresponding to large-scale changes in the trend of longshore velocities. However, there are no distinct peaks, so the effect of potential infragravity waves is not evident.

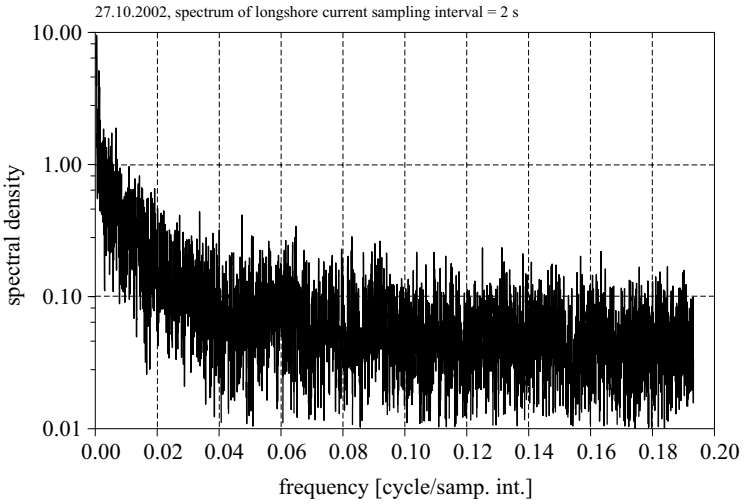

Fig. 4. Spectrum of longshore current time series

The longshore current series was decomposed into 100 RCs of the SSA method. This number was found to cover all the important patterns and was established by trial and error. Fig. 5 presents eigenvalues of this decomposition and shows that the first eigenvalue is more than one order of magnitude larger than the rest. Hence, the associated RC contains most information on this time series. Such a situation is frequently encountered when the SSA method is used; the trend can be extracted very easily, but the more delicate patterns require in-depth investigations and tedious scrutiny of the remaining eigenvalues and the associated RCs. Having *a priori* knowledge from the DWT study, we can assume that some useful information can also be stored in the eigenvalues 2 to 20, which depart somewhat from zero. Without this knowledge, the analysis of those quasi-residual eigenvalues would probably have been skipped. It therefore shows the superiority of the DWT method, which generates patterns when we proceed from high to low frequencies and assesses their importance from

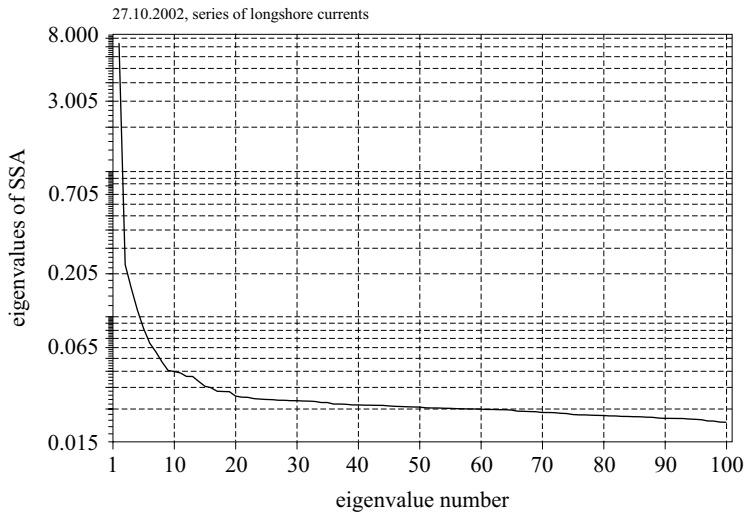

Fig. 5. Eigenvalues of SSA decomposition of longshore current series

their input to the total signal energy. In the case of the SSA method, discriminating between significant and insignificant eigenvalues on graphs like Fig. 5 is difficult and can lead to at least a superficial output. It is also worth noting that the remaining SSA eigenvalues are treated as a reflection of residual noise. In contrast, DWT does not discriminate between the patterns and noise but resolves the series into orthogonal spectral bands, proceeding from high to low frequencies. Hence, a dozen or so apparently insignificant SSA patterns can reflect a decent DWT pattern representing, for example, wind waves with $4 < T < 8$ s. Usually, though, it is very impractical to seek such subsets of a large number of RCs with little individual significance.

Fig. 6 presents the 1st RC (fine line) together with the trend extracted with DWT (cf. Różyński & Reeve, submitted). Both lines characterise the trend and are practically identical; their standard deviations are equal to 0.264 m s^{-1} for the DWT trend vs 0.27 m s^{-1} for its SSA counterpart. Therefore, DWT and SSA are equivalent as regards trend extraction: this is the most dominant series characteristic.

The extraction of further patterns turned out to be an arduous business. Fig. 7a presents the spectrum of the DWT pattern describing a spectral band, where the effect of the infragravity component with $T = 120$ s was sought. Such spectral bands are easily obtainable by simple high- and low-pass filtering of the series in question, starting from high down to low frequencies. As the emerging patterns are orthogonal and uncorrelated, their interpretation is relatively straightforward (Różyński

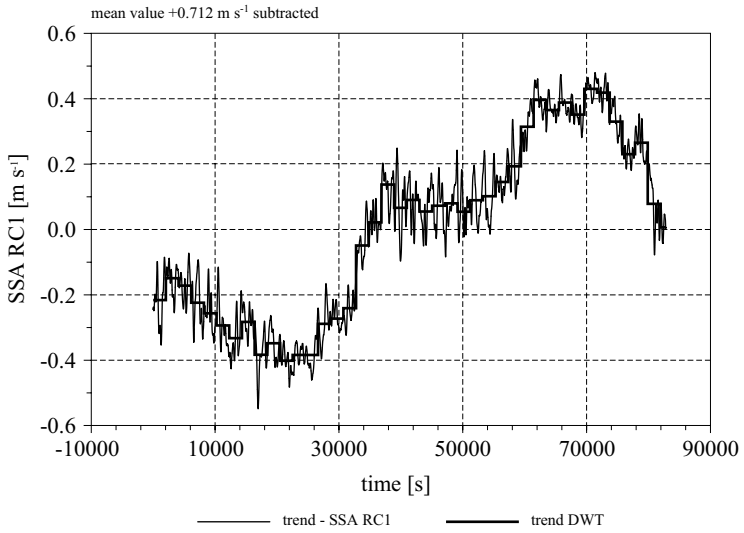

Fig. 6. Trend extracted with DWT and SSA methods

& Reeve, submitted). In contrast, the SSA reconstructed components are additive but non-orthogonal and correlated, so they require detailed scrutiny. Owing to the correlation of RCs, the patterns we are looking for are frequently contained in their subsets, which are usually searched for by trial and error. For this reason the graph in Fig. 7a provides substantial assistance for the SSA study, as it serves as reference for the best subset of RCs. The choice of this subset is illustrated in Figs 7b and 7c. The first choice was the subset of RC2 to RC8; this selection was based on the assessment of their individual spectra. However, the resulting spectrum, shown in Fig. 7b, revealed too much power in relation to the DWT analysis and was biased towards ultra-low frequencies. A much better fit was achieved by choosing the subset of RC4 to RC7, despite significant correlation between some of them and the removed RC2, RC3 and RC8 (see Table 3). Fig. 8 presents the potential infragravity component in the longshore current series for $T = 120$ s, obtained with the two methods: DWT (Fig. 8a) and SSA (Fig. 8b). Their magnitudes throughout the series show remarkable similarity, so that we can conclude that both methods were capable of revealing the same pattern. However, it should be added (i) that delicate patterns are contained in subsets of correlated RCs, which makes the whole analysis very time-consuming, and (ii) that the DWT method provides grounds for the proper selection of the best RCs subset. Without the prior knowledge from the DWT analysis, the SSA study would probably have remained inconclusive. This, in turn, suggests some superiority of

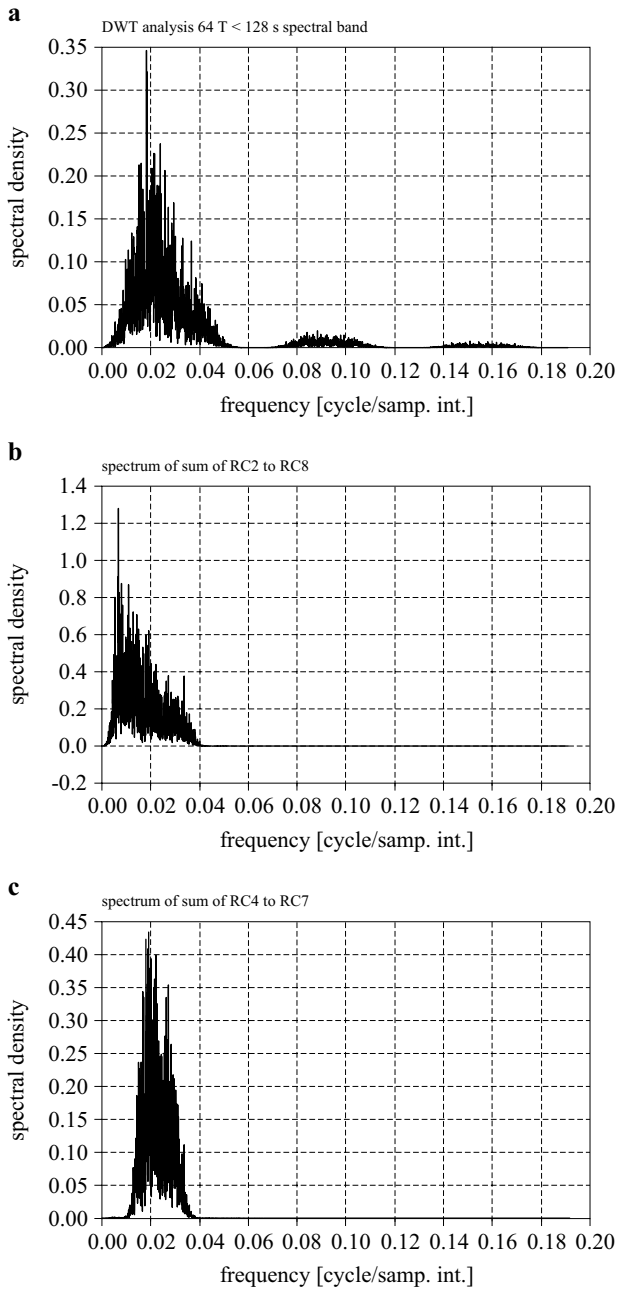

Fig. 7. Spectrum of the wavelet component for an infragravity wave with $T = 120$ s (a), sum of RC2 to RC8 (b) and sum of R4 to RC7 (c)

wavelet analysis over the SSA method when the composition of long hydrodynamic series are investigated.

The search for the second infragravity component with $T = 30$ s turned out to be even more tedious and somewhat more vague. First, the spectra of the remaining RCs, associated with eigenvalues from 11 to 20, were

Table 3. Correlations among RC2 to RC8

RC2	RC2	RC3	RC4	RC5	RC6	RC7	RC8
RC2	1	0.63	insignificant				
RC3		1	0.56	insignificant			
RC4			1	0.61	insignificant		
RC5				1	0.55	insignificant	
RC6		symmetry			1	0.66	insignificant
RC7						1	0.59
RC8							1

RC – reconstructed component.

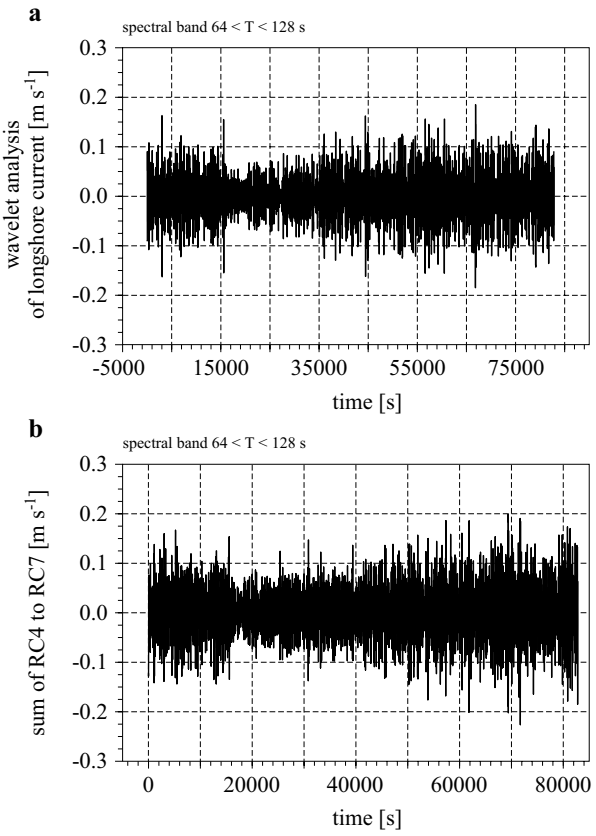

Fig. 8. Infragravity component $T = 120$ s reconstructed with DWT (a) and subset of RCs (b)

computed. They demonstrated that RC11, RC14, RC18 and RC19 were spectrally located about the period of $T = 30$ s. The peak period of the first two was just about 30 seconds, whereas the other pair displayed somewhat faster variations of 28 seconds. The other RCs were rejected, because their spectral locations were found to be too remote from the peak value of $T = 30$ s, despite some correlation with the retained elements (see Table 4).

Table 4. Correlations among RC11 to RC20

RC11	RC11	RC12	RC13	RC14	RC15	RC16	RC17	RC18	RC19	RC20
RC11	1	0.35	0.35	0.55	insignificant					
RC12		1	1.00	0.44	insignificant					
RC13			1	0.44	insignificant					
RC14				1	0.39	0.50	0.26	0.28	0.40	insignif.
RC15	symmetry				1	0.93	insignif.			0.43
RC16						1	0.39	insignif.		0.55
RC17							1	0.66	insignif.	0.41
RC18								1	0.75	0.33
RC19									1	0.31
RC20										1

RC – reconstructed component.

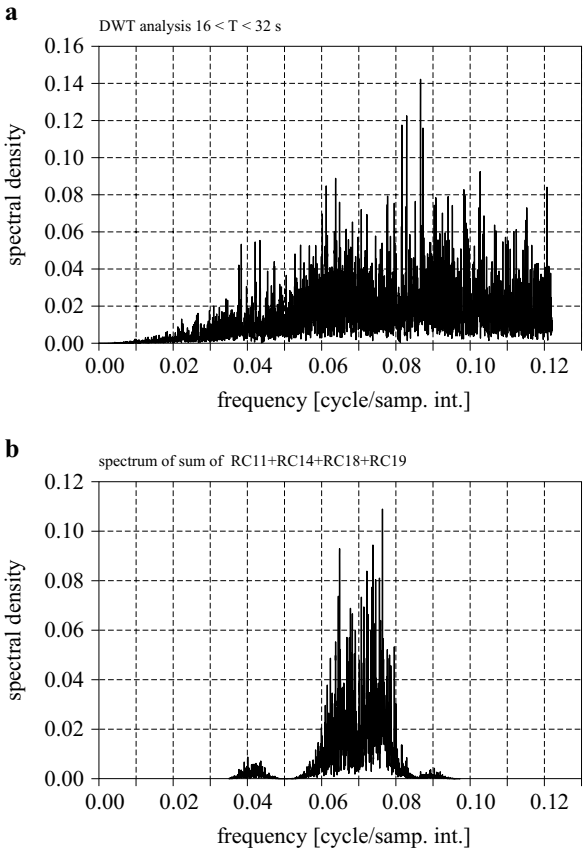

Fig. 9. Spectrum of the wavelet component for an infragravity wave with $T = 30$ s (a) and sum of RC11+RC14+RC18+RC19 (b)

The judgment whether a given component should be included or rejected is always arbitrary to some extent. Therefore, an ambiguity between the results of DWT and SSA emerged (see Figs 9 and 10). Fig. 9 shows the spectra of DWT and SSA output featuring the infragravity component with $T = 30$ s. It includes a much broader spectral band (Fig. 9a), especially towards higher frequencies ($16 < T < 32$ s). In contrast, the chosen SSA subset shows a much narrower band (Fig. 9b) with a substantially smaller energy input, which is confirmed by Fig. 10, where the trajectories of both reconstructions are plotted. These graphs illustrate the fact that DWT decomposition relies on fixed boundaries between spectral bands (Różyński & Reeve, submitted), which are strictly defined by the sampling rate, here 0.5 Hz. In other words, DWT is unable to discriminate between spectral components within a particular spectral band. On the other hand, the SSA method is capable of this, albeit at the expense of time-consuming and sometimes arbitrary manipulation of various reconstructed components. In connection with the considerations regarding the other infragravity component ($T = 120$ s), this indicates the synergistic nature of

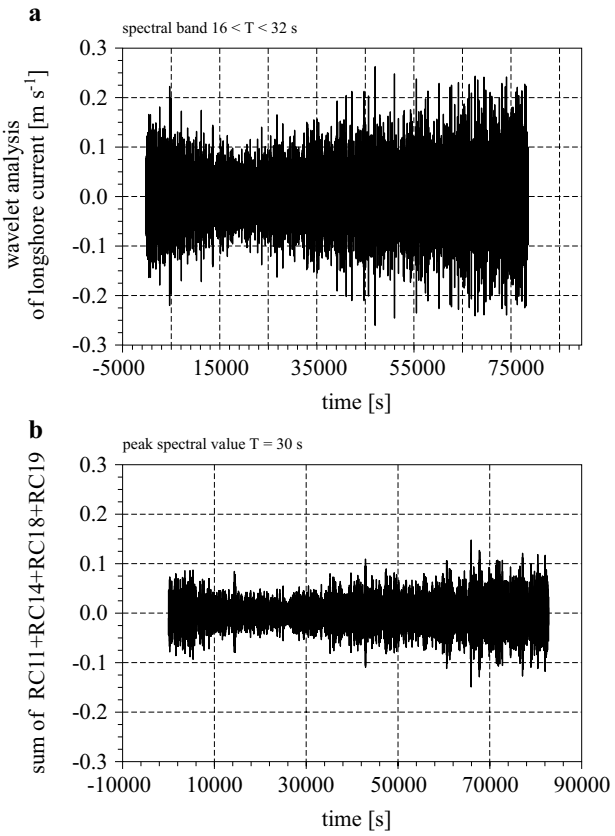

Fig. 10. Infragravity component $T = 30$ s reconstructed with DWT (a) and subset of RCs (b)

the two methods: DWT can provide a basis for pattern recognition, whereas with the SSA the patterns can be fine-tuned to pinpoint the phenomenon in question. Furthermore, as described previously, DWT can compensate for another drawback of SSA decomposition: it can provide an interpretation for the system dynamics stored in the residual RCs, here RC20+. In fact it was possible to assign physical explanations to almost all DWT patterns (Różyński & Reeve, submitted), whereas the system dynamics seen through the residual RCs was found to represent just residual noise.

In general, application of the SSA method yielded results similar to the DWT output. It brought little new information as regards the nature of the spectral bands located in the vicinity of low-frequency oscillations, and believed to represent the effects of infragravity waves. The presence of spectral components in the longshore current series, whose frequencies correspond to the frequencies of potential infragravity waves – progressive edge waves, is still only circumstantial evidence for their existence. Thus, further research on the extracted patterns of simultaneously recorded water levels and longshore currents is necessary for a better insight into their nature. It is planned to employ coherence functions in order to establish whether low-frequency oscillations of the water table and low-frequency variations of the longshore current are consistent enough to claim that the longshore current is perturbed by infragravity waves.

5. Conclusions

As is to be expected, the analysis of the same data set with two different signal processing methods is always complementary. Importantly, however, the time series analysed was a very long one, so it allowed for in-depth investigations of the performance of both methods, their merits and drawbacks, synergy and user-friendliness. The analysis found both methods to be good tools for studying nearshore hydrodynamics, since both were able to capture the key phenomena. Both methods revealed practically the same trend in the data, representing the growth of longshore velocities during the development of a stormy event. The ability of DWT to decompose the raw data into orthogonal and uncorrelated patterns, featuring spectrally disjoint bands, was found to be a convenient starting point for the SSA analysis, since it provided grounds for interpreting delicate SSA patterns that otherwise might have been ignored. Moreover, the reconstructed components of the SSA method are usually correlated, so when a long series is analysed, the selection of their relevant subset is a time-consuming trial and error procedure, unless the DWT output is available. All in all, this points to the superiority of DWT over SSA. Interestingly, though, we ought to speak about their synergy, because the SSA method can fine-tune the

rather crude DWT pattern, as happened with the infragravity component for $T = 30$ s. Still, DWT was found to be user-friendlier than SSA, because of the ease with which it can decompose a time series into patterns featuring various spectral bands. Theoretically, SSA is capable of that too, but from the practical point of view it is hardly possible, because of the large number of individually insignificant RCs, whose subsets can generate spectrally disconnected, but significant patterns. The large number of such RCs makes the choice of the right subset a mission impossible, unless the DWT output is known in advance.

The results of both methods as to the existence of infragravity waves remain inconclusive, although they may serve as circumstantial evidence supporting their presence. The extracted slow-varying components from both series will need further research to establish their mutual relationship. For this purpose, the analysis using coherence functions appears to be of particular interest, which indicates the direction that future research should take.

References

Aubrey D. G., Emery K. O., 1983, *Eigenanalysis of recent United States sea levels*, Cont. Shelf Res., 2 (1), 21–33.

De Vriend H. J., 1991, *Mathematical modeling and large-scale coastal behavior. Part 1. Physical processes*, J. Hydraul. Res., 29 (6), 727–740.

Ding X. L., Chao J., Zheng D. W., Chen Y. Q., 2001, *Long-term sea-level changes in Hong Kong from tide-gauge records*, J. Coast. Res., 17 (3), 749–754.

Huang M. C., 2004, *Wave parameters and functions in wavelet analysis with filtering*, Ocean Eng., 31 (7), 813–831.

Larson M., Kraus N. C., 1995, *Prediction of cross-shore sediment transport at different spatial and temporal scales*, Mar. Geol., 126 (1)–(4), 111–127.

Massel S., 2001, *Wavelet analysis for processing of ocean surface wave records*, Ocean Eng., 28 (8), 957–987.

Pruszak Z., Różyński G., Szmytkiewicz M., Ostrowski R., *Infragravity waves and rhythmic shoreline forms at a non-tidal, sandy coast with multiple bars*, Proc. 29th ICCE Conf., ASCE, Lisbon, (in press).

Pruszak Z., Różyński G., Szmytkiewicz M., Skaja M., 1999, *Quasi-seasonal morphological shore evolution response to variable wave climate*, Proc. Coastal Sediments ′99 Conf., ASCE, New York, 1081–1093.

Pruszak Z., Różyński G., Zeidler R. B., 1997, *Statistical properties of multiple bars*, Coast. Eng., 31 (1)–(4), 263–280.

Reeve D. E., 2002, *Comments on 'Forced and self organised shoreline response for a beach in the southern Baltic Sea determined through singular spectrum analysis'*, [Coast. Eng., 43 (2001), 41–58], Coast. Eng., 44 (3), 267–269.

Reeve D. E., Li B., Thurston N., 2001, *Eigenfunction analysis of decadal fluctuations in sandbank morphology at Great Yarmouth*, J. Coast. Res., 17 (2), 371–382.

Różyński G., 2003, *Data-driven modeling of multiple longshore bars and their interactions*, Coast. Eng., 48 (3), 151–170.

Różyński G., 2005, *Long-term shoreline response of a nontidal, barred coast*, Coast. Eng., 52 (1), 79–91.

Różyński G., Jansen H., 2002, *Modeling nearshore bed topography with principal oscillation patterns*, J. Waterw. Port Coast. Ocean Eng., 128 (5), 202–215.

Różyński G., Larson M., Pruszak Z., 2001, *Forced and self-organized shoreline response for a beach in the southern Baltic Sea determined through singular spectrum analysis*, Coast. Eng., 43 (1), 41–58.

Różyński G., Reeve D., *Multi-resolution analysis of nearshore hydrodynamics using discrete wavelet transforms*, Coast. Eng., (submitted).

Solow A., 1987, *The application of eigenanlysis to tide-gauge records of relative sea level*, Cont. Shelf Sci., 7 (6), 629–641.

Stive M., Aarninkhof S. J. C., Hamm L., Hanson H., Larson M., Wijnberg K., Nicholls R. J., Capobianco M., 2002, *Variability of shore and shoreline evolution*, Coast. Eng., 47 (2), 211–235.

Szmytkiewicz M., 2002, *Prądy pochodzenia falowego w morskiej strefie brzegowej (Wave-driven nearshore currents)*, IBW PAN Publ., Gdańsk, 1–235.

Vautard R., Yiou P., Ghil M., 1992, *Singular spectrum analysis: a toolkit for short, noisy and chaotic signals*, Physica D, 158, 95–126.

Wijnberg K. M., Terwindt J. H. J., 1995, *Extracting decadal morphological behaviour from high-resolution long-term bathymetric survey along the Holland coast using eigenfunction analysis*, Mar. Geol., 126, 301–330.

Winant C. D., Inman D. L., Nordstrom C. E., 1975, *Description of seasonal beach changes using empirical eigenfunctions*, J. Geophys. Res., 80 (15), 1979–1986.

Appendix

Symbols used in the text

Symbol	Denote
a_i^k	i-th element of k-th SSA principal component, $i = 1,\ldots,N - M + 1$
$c(j)$	covariance for lag j
D_{50}	mean sediment grain size
E^k	eigenvectors of T_x, $k = 1,\ldots M$
H_s, $\overline{H}$, H_0	respective wave heights: significant, average and deepwater
h	water depth
L_0	deepwater wavelength
M	window length in SSA, M-1 maximum lag included
N	length of x
$\tan\beta$	mean seabed slope
T	period, $\omega = 2\pi/T$
T_x	matrix of lagged covariances: SSA system matrix
x	analyzed time series
x^k	k-th reconstructed component (RC)
λ_k	eigenvalues of T_x, $k = 1,\ldots \mathrm{M}$
ξ	surf similarity parameter